Fuel 102 (2012) 256–263

Contents lists available at SciVerse ScienceDirect

Fuel

journal homepage: www.elsevier.com/locate/fuel

The fluidization behaviour of torrefied biomass in a cold model

Patrick Rousset [a],*, Thomas Petithuguenin [b], Thiago Rodrigues [c], Ana-Cristina Azevedo [d]

[a] UPR 42 Biomass Energy, French Agricultural Research Centre for International Development (CIRAD), Brasilia DF 70818-900, Brazil
[b] INSA, Department of Energetic and Environmental Engineering, Lyon, France
[c] Forest Sciences Department, Brasilia University, Brazil
[d] Laboratory of Forest Products, Brazilian Forest Service (LPF-SFB), Brasilia DF 70818-900, Brazil

HIGHLIGHTS

- Hydrodynamics play a crucial role in defining the performance of fluidized beds.
- Improvement of fluidization through torrefaction is a pre-treatment option.
- The pressure drop was mainly affected by particle size.
- Interaction between static bed height and temperature not affect the final results.

ARTICLE INFO

Article history:
Received 23 February 2011
Received in revised form 18 October 2011
Accepted 3 July 2012
Available online 20 July 2012

Keywords:
Hydrodynamics
Torrefaction
Fluidization
Biomass
Sawdust

ABSTRACT

This experiment proposes a methodology to study the fluidization properties of torrefied biomass. The need for the experiment was highlighted by the impossibility of predicting the behaviour of amorphous, multi-dimensional biomass particles, despite the existence of the kinetic theory of granular flows related to fluidization. The tests were carried out in a cold flow fluidization bed chamber with an internal diameter of 150 mm, with air as the fluidizing medium, and a chamber height of up to 750 mm. Bed-pressure drop was measured as a function of superficial air velocity over a range of bed heights for each individual type of particle. The results showed that the pressure drop was mainly affected by particle size. Interaction between static bed height and temperature did not significantly affect the final results.

© 2012 Elsevier Ltd. All rights reserved.

1. Introduction

Biomass can be used to produce energy by different technologies: thermochemical (combustion and gasification), biological (anaerobic digestion and fermentation) or chemical (esterification) processes [1]. However, biomass in its original state has a wide range of moisture contents, low bulk density and low energy density and is difficult to transport, handle, store and feed into the existing industrial systems. Torrefaction is a process that converts diverse lignocellulosic biomass feedstocks into an energy-dense homogeneous solid, as a pre-treatment for subsequent thermochemical conversion. This thermal treatment, also called mild pyrolysis, involves the heating of biomass at moderate temperatures (200–280 °C) under an inert atmosphere [2]. The main changes in biomass due to torrefaction are the decomposition of hemicelluloses, and partial depolymerisation of lignin and cellulose [3]. As a means of woody biomass fuel upgrading, torrefaction thus produces a fuel with a faster combustion rate, less smoking and fewer hydrophobic characteristics [4]. The final product yields (solid, liquid, and gas) are strongly dependent on the torrefaction temperature, reaction time and biomass type [5]. The torrefied wood is more brittle with much better milling properties. It has been shown that torrefaction decreases both grinding energy and particle size distribution [6].

The chief advantage of fluidization is that the solid is vigorously stirred by the fluid passing through the bed, so the boundary layers of the fluid are broken and mixing of the solid ensures that there are practically no temperature gradients in the bed, even with quite exothermic or endothermic reactions [7]. However, biomass particles have unusual properties which make them difficult to fluidize and handle because of high cohesion forces between the particles and channelling [8]. In itself, fluidization can also lead to the attrition of solid particles. Because of attrition, the size of the solid particles is reduced and the possibility of entrapping solid particles with the fluid is greater. Improving the fluidization properties of biomass through torrefaction is seen as a promising pre-treatment

---

* Corresponding author. Tel.: +55 61 2028 7231; fax: +55 61 2028 7199.
E-mail address: patrick.rousset@cirad.fr (P. Rousset).

0016-2361/$ - see front matter © 2012 Elsevier Ltd. All rights reserved.
http://dx.doi.org/10.1016/j.fuel.2012.07.007

Nomenclature

Δp	pressure drop (Pa)
P_{sat}	saturation pressure (Pa)
L	bed thickness (m)
h	head loss (m)
$\Delta h_{equipment}$	head loss due to the equipment (m)
Z	elevation of the point above a reference plane (m)
V	air speed (m s^{-1})
V_{mf}	minimum fluidization velocity (m s^{-1})
$V_{settling}$	terminal velocity (m s^{-1})
V_{opt}	maximum fluidization velocity (m s^{-1})
S_p	particle surface (m^2)
V_p	particle volume (m^3)
D_p (ESD)	equivalent spherical diameter (m)
fp	friction factor (dimensionless)
Gr	Grashof number (dimensionless)

Greek symbols

φ	particle sphericity
Φ	relative humidity (%)
$\rho_p \rho_s$	particle density (kg m^{-3})
ρf	fluid density (kg m^{-3})
ρ	fluid (air) density (kg m^{-3})
ε	void content (dimensionless)
ε_{mf}	void content at minimum fluidization (dimensionless)
μ	fluid dynamic viscosity (Pa s)

option for implementation in pulverised systems, such as cofiring with coal in large-scale utility boilers or large-scale (entrained-flow) gasification of biomass [9]. The fluidization and pneumatic transport properties of small, torrefied wood particles would appear to be much better than those of corresponding small wood particles, and their behaviour resembles that of dry coal particle fluidization [10].

Previous studies have focussed on the loss of mass during biomass torrefaction [11] (Repellin, 2010#606), the effect of processing conditions on the chemical properties of the product [12], or the grindability and reactivity [13,14] of torrefied biomass. Less attention has been paid to raw biomass fluidization and to heat-treated biomass depending on torrefaction processing conditions and particle size [15].

The purpose of this work was to study changes in the cold fluidization behaviour of *Eucalyptus* sp. biomass before and after treatment at 200 °C for 15 min. Fluidization, depending on the processing conditions and the particle size of raw biomass, was evaluated using a cylindrical chamber. Air flow and pressure drop were determined by multiple pressure loss measurements through the bed of biomass, in order to specify the optimum flow velocity of the heat transfer gas through the biomass. The effect of superficial velocity, immersion depth and granular properties (size and density) on the incipient fluidization point was investigated. An analysis of variance was used to test for particle size, bed height and treatment group differences.

The torrefaction technologies available include continuous and fixed-bed batch processes. The findings in this study could be used to design or improve those technologies.

2. Materials and methods

2.1. Raw material

Eucalyptus sp. sawmill waste was used as the raw material. The samples were torrefied using a lab-scale reactor as described in Rodrigues and Rousset [16]. The samples used to study fluidization behaviour were dried beforehand at 103 °C for 48 h and placed in a reactor under nitrogen and heated to 200 °C for 15 min. Different particle size groups were selected based on the composition of the raw material. Wood chips were passed through different sieves to obtain the adequate granulometry before the experiments. Three particle sizes that were the most representative in mass proportion were obtained from the mixture: $X_1 < 0.3$ cm (21.25%), $0.3\text{ cm} < X_2 < 0.5$ cm (48.63%) and $0.5\text{ cm} < X_3 < 1.3$ cm (27.12%). Above 1.3 cm, the mass proportion was less than 3%. The fluidization study was carried out on raw biomass and treated biomass for each particle size group and the mixture (Fig. 1).

2.2. Process description

A special device (Fig. 2) was designed and built to measure pressure drop depending on the physical characteristics (untreated, treated, and particle size) of the biomass. The fluidized lab-scale reactor consisted of a batch type flexi-glass fluidizing column of approximately 750 mm in length with an internal diameter of 150 mm in which the biomass was placed for fluidization and observation. It was equipped with filters at the bottom and top. The air was provided by a blower (a 0–60 Hz synchronous electric motor) coupled to the fluidizing column by flexible ducts, from which the outflow was controlled by a frequency inverter (WEG, CFW-08 for speed control of three-phase induction motors) with a programmable output frequency. It should be borne in mind that, at a given frequency, air flow can vary depending on pressure loss in the circuit. The output frequency had a precision of 0.01 Hz. An anemometer (Instrutemp Itan 720) measured the air speed (imprecision of ±2% with a 0.1 resolution digit) at the reactor outlet – the internal diameter was 59.5 mm. Flexible tubings and valves completed the circuit. A mechanical stirring device was used to enhance fluidization efficiency at the bottom. A motor was located under the bottom filter, giving the incoming air a radial velocity (as opposed to its purely axial entry).

Bed pressure drop was measured while increasing the velocity through the bed for height (70, 100, and 150 mm). Minimum fluidization was categorised by visually observing the bed at a given moment of fluidization after bed expansion. Air temperature was measured during the run. The temperature of the air changed and so therefore did its density; primarily, excess heat was provided by the blower. At a given moment, it was considered that the air temperature was constant in the circuit; it was measured by the anemometer and the imprecision was ±1 smallest digit. For pressure measurements, a U-manometer was used giving data in mm_{H2O} (reminder: 1 cm H_2O = 98.0638 Pascals = 98.0638×10^{-5} Bar).

2.3. Pressure drop measurement

An expanded bed has some of the properties of a fluid and is also called a fluidized bed [7]. As the air speed (V) increases, the void content of the bed may increase and keep the pressure drop (Δp) constant. The bed height (L) will also increase, but its effect is much less than the effect of change in ε. For velocities under the minimum fluidization velocity (V_{mf}), the bed behaves as a

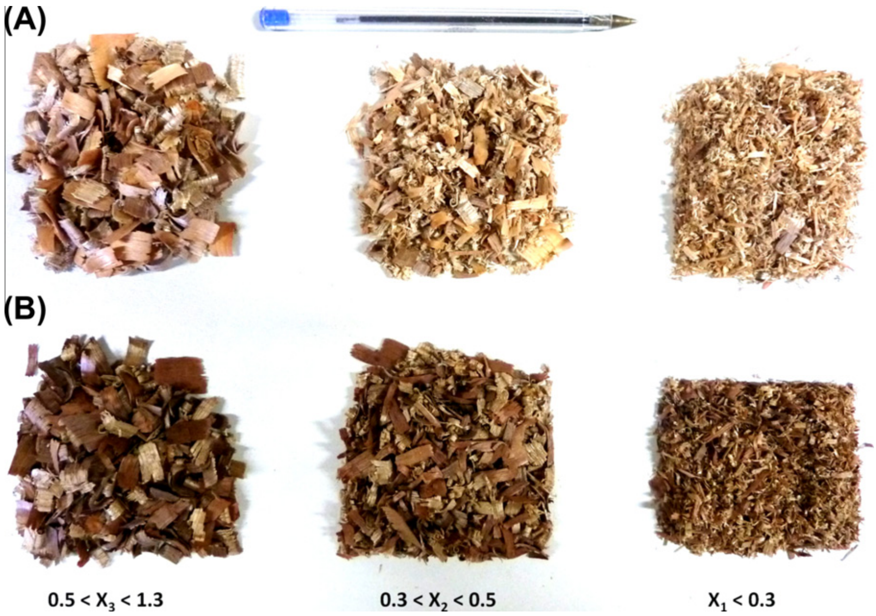

Fig. 1. Different particle size (cm) groups. (A) Before treatment and (B) after treatment at 200 °C, 15 min.

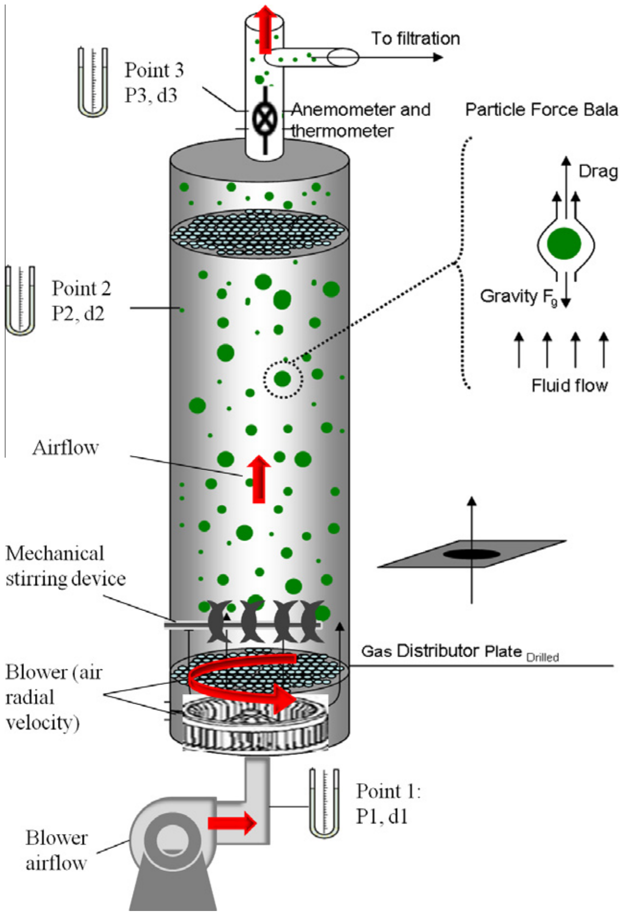

Fig. 2. Experimental devices to measure the pressure drop across the bed.

packed bed. However, as the velocity is increased past V_{mf}, not only does the bed expand (L increases), but also the particles move apart, and (ε) also increases to keep the (Δp) constant.

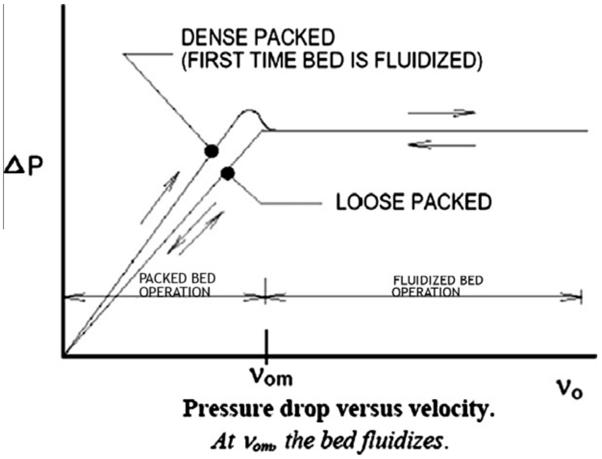

Fig. 3. Pressure drop versus velocity. This graph shows that the relationship between pressure drop and velocity is dependent on the conditions of the packed bed – densely packed versus loosely packed. The point where the increasing and decreasing curves meet (or alternatively the breaking point in the pressure curve) corresponds to the incipient fluidization speed, which is also, in theory, the ideal speed for gas/particle heat transfer.

Beds of solids fluidized with air usually exhibit what is called aggregative or bubbling fluidization. At superficial velocities much greater than V_{mf} most of the gas passes through the bed as bubbles or voids which are almost free of solids, and only a small fraction of the gas flows in the channels between the particles. As the velocity is further increased, the bed becomes increasingly expanded, and the solid content becomes increasingly dilute. Finally, the velocity becomes as great as the terminal settling velocity (V_t) of the individual particles, so the particles are blown out of the system. Thus, the velocity range for which a fluidized bed can exist is from V_{mf} (can be calculated from Eq. (5)) to V_t. For spherical particles, the pressure drop curve appears as displayed in Fig. 3.

To measure pressure drop, a known amount of biomass, for which the exact mass, effective density and void proportion ε were known, was placed in the tube. The air flow was gradually increased and the pressure values were recorded. So far, one value for every 3 Hz has been used, but graphs indicate smaller steps would be better.

Two things were expected:

- Pressure loss as a function of bed height should be linear in the pre-incipient regime (with pressure loss at the origin being that of the distributor). This is because pressure loss due to friction forces is a linear function of velocity squared (V^2) and length, and ΔP is approximately a function of V^2 before the incipient point.
- V_{opt} (as the various particle sizes will procure various values of Vf, the greatest should correspond to V_{opt}) should be constant; if not, a rule of dependency should be deduced from further measurements.

As already known, a mixture of biomass particles comprises many different particle sizes, which have different fluidization and settling speeds. As the experiments proceeded, it was noticed that the smaller particles had settling speeds that were lower than the minimum fluidization speeds for larger particles. The effect was that as the air velocity was increased, more and more particles reached their settling velocities and were carried away. Thus, an increasing number of particles remained stuck on the upper filter of the column. Not only was this not desirable on a practical level (the aim was a fluidized bed, not a partially fluidized bed and a layer of particles stuck above it), but it made pressure readings difficult to analyse as the pressure loss due to particles stuck under the top filter was high and increased rapidly. An extra pressure measurement was therefore taken under that layer at point 2 (Fig. 2).

2.4. Applicability of the kinetic theory of granular flows

The kinetic theory of granular flows enables predictions for the fluidization of solid beds and heat transfer in granular flows with spherical (or quasi spherical) particles. However, it is largely impossible to make these predictions or simulate flows with biomass particles due to the amorphous nature of biomass, multiple particle sizes, low sphericity and acute angles. An experimental study was therefore necessary.

The study needed to encompass as many types of particles and biomass as possible, but on this pilot scale it was limited to two batches of wood chips (Chips 1 and 2), both from eucalyptus. The formulas were also applied to a batch of bamboo fibres (Chips 3). An average particle was picked out from each batch and the particle dimensions were measured using a calliper. The mass of particles selected was measured with an appropriate balance (Table 1).

The Ergun equation [18] expresses the friction factor in a packed column as a function of the Reynolds number:

$$f_p = \frac{150}{Gr_p} + 1.7555 \text{ and } Gr_p = \frac{150(1-\varepsilon)\mu}{D_p V_s \rho} \qquad (1)$$

$$f_p = \frac{\Delta p}{L}\frac{D_p}{\rho V^2}\left(\frac{\varepsilon^3}{1-\varepsilon}\right) = \frac{150(1-\varepsilon)\mu}{D_p V_s \rho} + 1.75 \qquad (2)$$

where Δp is the pressure drop across the bed, L is the bed length (not the column), D_p is the equivalent spherical diameter of the packing, ρ is the fluid density, μ is the fluid dynamic viscosity, V_s is the superficial velocity (i.e. the velocity that the fluid would have through the empty tube at the same volumetric flow rate), and ε is the void fraction of the bed (bed porosity at any time).

Table 1
Biomass particle characteristics used to estimate the applicability of the kinetics theory of granular flow. Chips 1 and 2 were from Eucalyptus, Chips 3 from Bamboo.

	Chips 1	Chips 2	Chips 3
Particle density, ρ_p (kg m^{-3})	58.6	52.647	86.757
Particle surface, S_p (m^2)	2.40E−04	3.69E−04	5.87E−04
Particle volume, V_p (m^3)	1.00E−07	1.38E−07	2.33E−07
Particle sphericity, φ	0.434	0.349	0.312

Table 2
Minimum fluidization velocity (V_{mf}) calculated by the Ergun equation and settling velocity (V_t) estimated using the Ganser correlation. V_{mf} was greater than V_{settling} in two cases. Chips 1 and 2 were from Eucalyptus, Chips 3 from Bamboo.

	V minimum fluidization (V_{mf})			$V_{settling}$ (V_t)
	Eq. (3)	Eq. (4)	Eq. (5)	
Chips 1	0.200	0.101	0.364	0.450
Chips 2	0.161	0.081	0.364	0.359
Chips 3	0.251	0.143	0.512	0.448

Three simplified forms of the Ergun equation were used to calculate the minimum fluidization velocity (V_{mf}); the first and second were for spheroids, and the third for less spherical large feed particles. The reader will find a complete examination to evaluate the accuracy of the Ergon equation in [17].

Simplified forms of the Ergon equation:

$$V_{mf} = \frac{(\rho_p - \rho_f) g D_p^2 \varepsilon^3}{150\mu(1-\varepsilon)} \qquad (3)$$

$$(\rho_p - \rho_f) g = 150 \frac{(1-\varepsilon_{mf}) g D_p^2 \varepsilon^3}{\varepsilon_{mf}^3} \frac{\mu V_{mf}}{(\phi d_p)^2} + 1.75 \frac{\rho_f V_{mf}^2}{\varepsilon_{mf}^3 \phi d_p} \qquad (4)$$

$$V_{mf}^2 = \frac{\phi d_p(\rho_s - \rho_f)}{1.75\rho_f} g \varepsilon_{mf}^3 \qquad (5)$$

As for the settling velocity (V_t), the Ganser correlation was used [8], which involves two shape factors and the drag coefficient. The results are summarized in Table 2. The results showed that the existing correlations did not apply to the biomass particles in this study (there are two cases in which V_{mf} was greater than $V_{settling}$) and highlighted the need for experimentation.

2.5. Air density

The calculation of air density ρ was very important in this study as the circulating fluid temperature varied; it was assumed that the ambient humid air was a perfect gas and that the following equation (Eq. (6)) was therefore true:

$$\rho = p / R_h T \qquad (6)$$

The gas constant of humid air can be expressed as a function of the dry air gas constant (R_s = 287.06 J kg^{-1} K^{-1}), water vapour gas constant (R_v = 461 J kg^{-1} K^{-1}), the relative humidity (φ, which in the dry early August weather in Brasilia was approximately 0.4), the saturation pressure (P_{sat}) and the total air pressure (P) as follows:

$$R_h = \frac{R_s}{1 - (\phi.P_{sat}/p)(1 - R_h/R_v)} \qquad (7)$$

P_{sat} can then be expressed with the Magnus formula [19], valid between −30 °C and +70 °C:

$$P_{sat} = 611.657 \exp\left(17.2799 - \left(\frac{4102.99}{(\vartheta + 273.15) - 35.719}\right)\right) \qquad (8)$$

Giving the global equation, with temperatures in °C and pressures in Pa:

$$\rho(\phi,\vartheta,p) = \frac{1}{287.06(\vartheta + 273.15)}\left(p - 230.617\vartheta \exp\left(\frac{17.5043\vartheta}{241.2^\circ C + \vartheta}\right)\right) \qquad (9)$$

2.6. Statistical analysis

O Time-series analyses of in-bed fluctuation signals, such as pressure and voidage signals, have been used in the past decade in fluidized beds to characterise flow behaviour. Time-series signals can be analysed in three different ways: statistical analysis, frequency analysis and chaotic analysis, in which the statistical analysis is the simplest and the most frequently employed. The most frequently studied quantities in dynamic analyses of gas–solid fluidized beds are pressure fluctuations [20].

One of the main applications of ANOVA is multiple comparison testing designed to check whether or not the parameters for the various categories of a factor differ significantly. Numerous tests have been proposed for comparing the means of categories. Tukey's test is the most used (HSD: Honestly Significant Difference). It is a single-step multiple comparison procedure and statistical test generally used in conjunction with an ANOVA to find out which means are significantly different from one another. The test compares the means of every treatment to the means of every other treatment, i.e. it applies simultaneously to the set of all pairwise comparisons and identifies where the difference between two means is greater than would be expected to be allowed by the standard error. If only pairwise comparisons are of interest, and all factors have equal sample sizes, Tukey's method gives shorter confidence intervals and is thus more powerful [21]. XLSTAT [22] is a modular statistical software used in this study. It relies on Excel for data inputting and result displaying, but the computations are made using autonomous software components.

3. Results and discussion

3.1. Calibration graph

In fluid dynamics, head is a concept that relates the energy in an incompressible fluid to the height of an equivalent static column of that fluid. From Bernoulli's Principle, the total energy at a given point in a fluid is the energy associated with the movement of the fluid, plus energy from pressure in the fluid, plus energy from the height of the fluid. The intention was to study pressure loss due to the biomass. It was therefore first necessary to know the pressure loss due to the equipment ($\Delta h_{equipment}$), according to the Bernoulli equation [23]:

$$\frac{P_1}{\rho g} + Z_1 + \frac{v_1^2}{2g} = \frac{P_3}{\rho g} + Z_3 + \frac{v_3^2}{2g} + \Delta h_{biomass} + \Delta h_{equipment} \tag{10}$$

The experiment was run without biomass to find the equation governing $\Delta h_{equipment}$. Considering pressure loss to be the convention (meaning it is positive) and with all constants being positive, this gave:

$$\frac{\Delta P_{3-1}}{\rho g} = \Delta h_{equipment} - \Delta z \tag{11}$$

$$\Delta h_{equipment} = \frac{k}{2g} v^2 - \frac{\omega m}{\rho} \tag{12}$$

$\frac{k}{2g} v^2$ is called the velocity head, expressed as a length measurement. It represents the energy from the height of the fluid lost by the addition of singularities arising from the equipment. $\frac{\omega m}{\rho}$ represents the energy from the height of the fluid provided by the small blower situated under the bottom filter between points 1 and 3 (Fig. 2). This thus gave:

$$\Delta P_{3-1} = \rho\left(\frac{k}{2} v^2 - \frac{g \omega \pi d^2}{4} v\right) - \Delta z \tag{13}$$

Or simply:

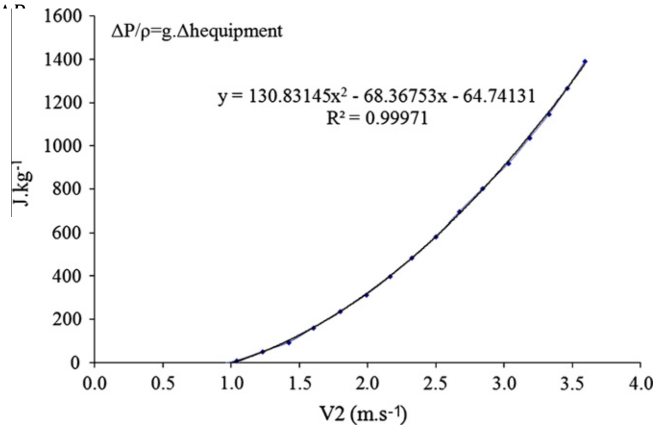

Fig. 4. Calibration curve: specific energy ($\mathrm{J\,kg^{-1}}$) as a function of velocity V2 ($\mathrm{m\,s^{-1}}$).

For all the experiments, a $\Delta P = f(V)$ graph was created as a function of bed height, untreated and treated biomass, and particle size. The regime changes and V_{opt} were recorded for the incipient fluidization point. As the various particle sizes procured various Vf values, the greatest corresponded to V_{opt}. The first sets were carried out on a mixture of untreated eucalyptus wood chips comprising many different particle sizes. Three bed heights were chosen (7 cm, 10 cm and 15 cm). Pressure loss was converted from cm H_2O to Pa and the influence of the equipment was deduced from the total pressure difference. Fig. 5 superposes the visual accounts with occurring events in the bed. The $\Delta P = f(V)$ graphs showed that the fluidized bed evolved as though it comprised various batches of particles (which was the case) – the interesting thing being that the behaviour of these batches could be observed. Thus, the three zones of incipient fluidization corresponded to air speeds (V) between 1.80–1.93, 2.08–2.22 and 2.36–2.77 $\mathrm{m\,s^{-1}}$ respectively For the rest of this study, it was assumed that these three zones corresponded to the behaviours of the main three particle groups ($X_1 < 0.3$ cm (21.25%), 0.3 cm $< X_2 <$ 0.5 cm (48.63%), 0.5 cm $< X_3 <$ 1.3 cm (27.12%)). Indeed, aligning the graphs with visual observations showed that when a batch of particles reached incipient fluidization, the pressure loss stagnated (as velocity rose), whereas when a batch reached settling speed, it was carried in the flow, remained stuck under the top filter, created a thick layer, and thus led to a rapid increase in pressure loss (with regard to air velocity), as shown in Fig. 5. All the graphs have been grouped according to bed height in Fig. 6.

An analysis of variance was performed to estimate the "bed height" effect on the pressure losses observed and to differentiate between the values obtained for the three bed heights. The results are given in Table 3. The statistical study confirmed that two groups (a and b) were obtained, where the values found for the 7 and 10 cm beds were not significantly different. For the rest of this study, two bed heights were therefore adopted: 10 and 15 cm.

Fig. 7 displays the total pressure lost versus velocity as a function of particle size, the treatment (untreated and treated biomass) and the bed height. The pressure drop was found to decrease as the particle size increased. For each bed height, two groups of curves could be distinguished. The first corresponded to the lowest granulometry ($X_1 < 0.3$ cm), whereas the second group corresponded to the other two particle sizes. The maximum values varied from 77.13 Pa to 305.9 Pa, all variables combined. Using these values, a multivariate analysis was carried out to determine those that were significantly different. The results are given in Fig. 8. Four groups of values were obtained, the highest being attributed to the lowest particle size ($X_1 < 0.3$ cm).

Tukey's test was also used to compare the means of each treatment to the means of every other treatment, in order to find out

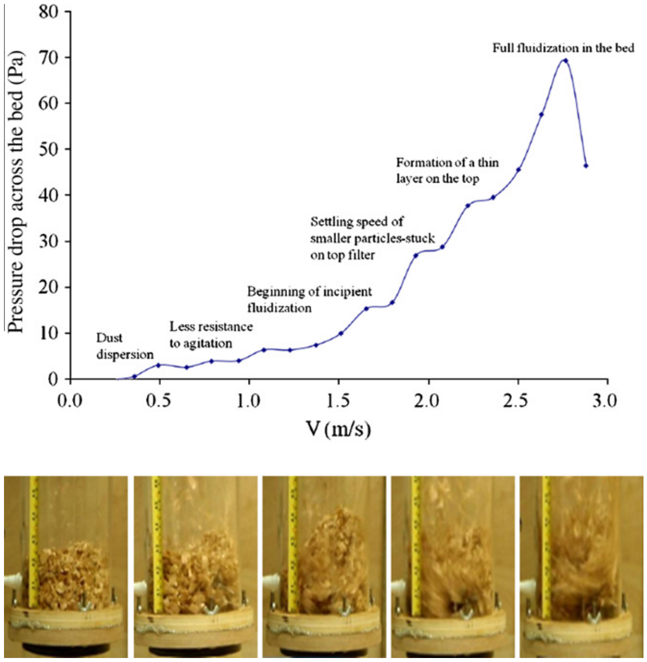

Fig. 5. Total pressure drop between points 1 and 3 due to untreated biomass for a 10 cm bed height with a description of events and visual observations.

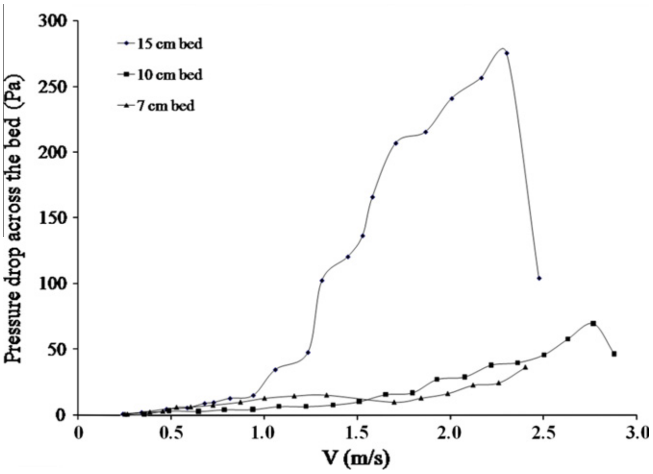

Fig. 6. Total pressure loss between points 1 and 3 due to untreated biomass in all the beds (7, 10 and 15 cm).

Table 3
Multivariate analysis of pressure drop versus bed height. For each group, the means with the same letter were not significantly different at 5% ($\alpha = 0.05$).

Bed (cm)	Pressure drop (Pa)			
	Minimum	Maximum	Mean	Standard deviation
7	0.460	36.075	11.546b	9.448
10	0.545	69.308	20.289b	21.244
15	0.562	275.460	93.448a	97.825

which means were significantly different from one another. The results are shown in Fig. 9. Two statistical groups were identified.

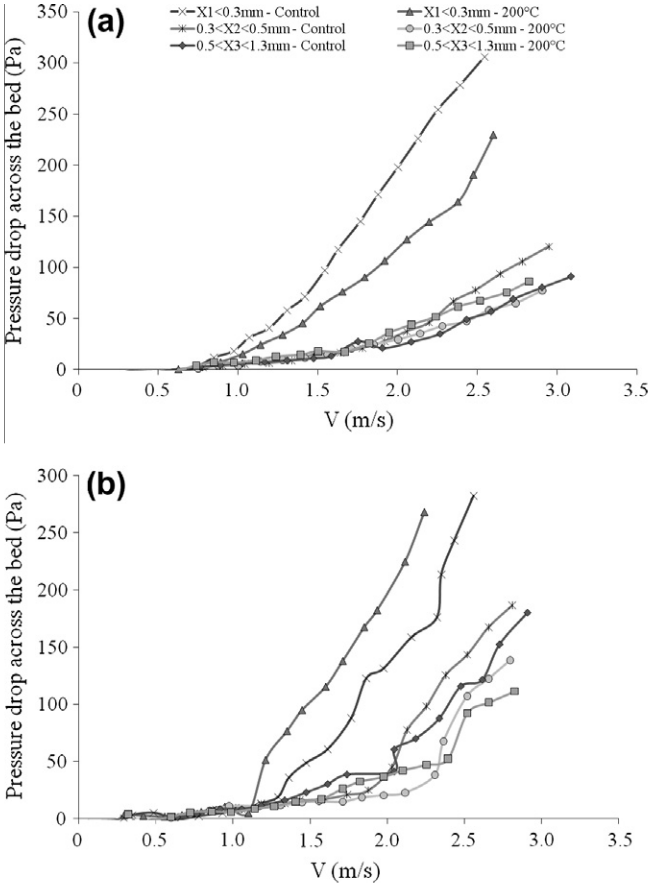

Fig. 7. Total pressure loss due to untreated and treated biomass versus particle size, (a) is a 10 cm bed height and (b) is a 15 cm bed height.

The pressure drop tendency for untreated biomass was also found to be generally higher than for treated biomass at the same velocity, except for the 15 cm bed and $X_1 < 0.3$ cm. Up to $V = 2$ m s^{-1}, the pressure drop was greater for the 15 cm bed; over 2 m s^{-1}, there were no significant differences. For small particle sizes ($X_1 < 0.3$ mm), the pressure drop increased earlier for small velocities in comparison with larger particle sizes. It was more evident for the 10 cm bed height.

Type III sum of squares analyses were carried out to determine which parameters significantly interfered ($\alpha = 0.05$) with the pressure drop and the air velocity, along with the effect of second and third order interactions. Of the parameters studied, size was the only factor with a significant impact on pressure drop. The interaction between size and treatment, size and bed, and finally size and bed and treatment, did not provide any significant response in either pressure drop or air velocity. The *P*-values are listed in Table 4.

An examination of the videos of the bed showed it to be made up of numbers of constantly forming, dissolving, and shifting channels. The superficial velocity for both the 10 and 15 cm static bed heights had to be increased to about 2.7 m s^{-1} for the bed pressure drop to equal its original weight. Other work on rice husk fluidization obtained the same results with a superficial velocity of 3.7 m s^{-1} [24].

4. Conclusion

The behaviour of biomass in a fluidized bed, with a wide range of granular biomass properties, was investigated. The effect of the superficial velocity, immersion depth, and granular properties (size and density) on the incipient fluidization point was investigated. The air flow and pressure drop were calculated via multiple pressure loss measurements through the bed of biomass in a cylindrical chamber. The tendency showed a greater pressure drop for

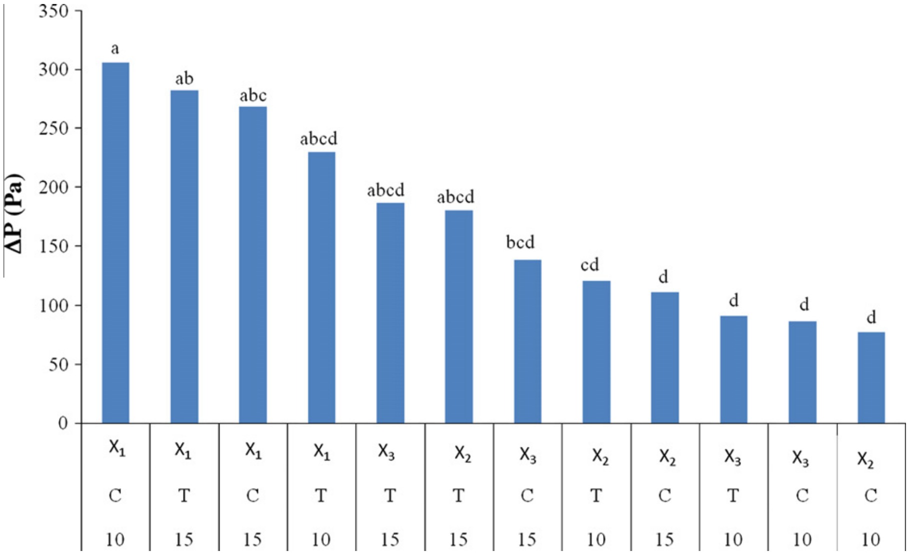

Fig. 8. Classification by Tukey's test in decreasing order for the higher value of the ΔP response variable. The values with the same letter were not significantly different at 5% ($\alpha = 0.05$). C = control, T = torrefied.

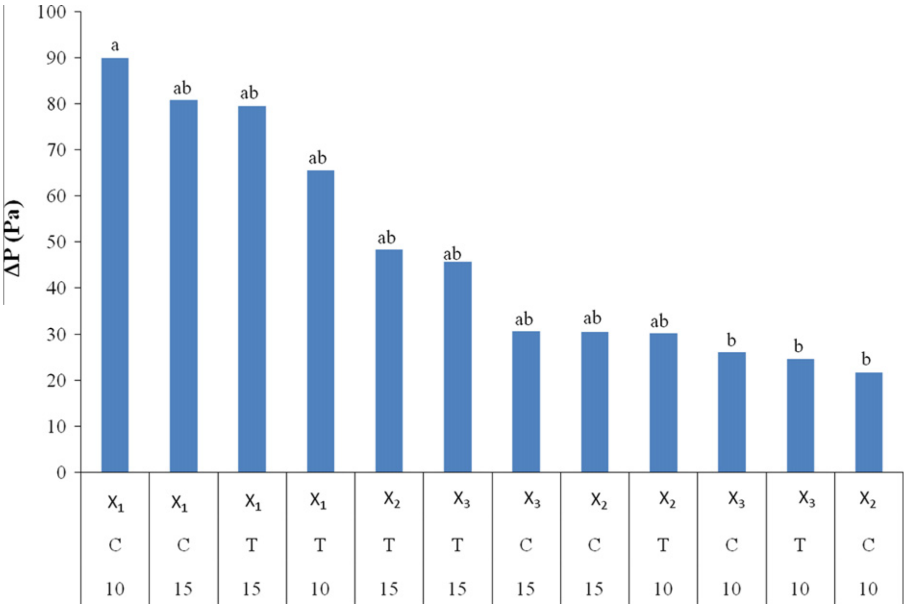

Fig. 9. Averaged results for the response variable ΔP (Pa). The means with the same letter were not significantly different at 5% ($\alpha = 0.05$). C = control, T = torrefied.

Table 4
Analysis of variance for Bed height (B), Treatment (T) and Particle Size (S) parameters, along with their first, second and third order interactions for the variables analysed (pressure drop and air velocity).

	Bed (B)	Treatment (T)	Size (S)	($B \times T$)	($B \times S$)	($T \times S$)	($B \times T \times S$)
Pressure drop (Pa)	ns *0.222*	ns *0.760*	* *<0.0001*	ns *0.298*	ns *0.815*	ns *0.377*	ns *0.936*
Air velocity (m s^{-1})	ns *0.859*	ns *0.938*	ns *0.218*	ns *0.560*	ns *0.962*	ns *0.842*	ns *0.764*

ns = Not significant at 5%. The *p*-values are in italics. Only the particle size impacted on the pressure drop.
[*] Significant at 5%

untreated biomass than for treated biomass at the same velocity. Raw biomass has poor grindability. After torrefaction, grindability characteristics are improved when compared to raw biomass; the biomass is weakened, which results in a reduction in pressure drop. The level of biomass destruction can be determined by sieving and analysing the size distribution of the fragments. Another study is under way and should be published soon.

The pressure drop also decreased as the particle size increased. The statistical analysis showed that the static bed height between 7 and 10 cm and the heat treatment had no significant impact on the pressure drop, which was mainly affected by the particle size. Our results could be used on a cold model circulating fluidized bed [25].

Acknowledgement

The authors would like to thank Prof. Gurgel, Director of the Department of Mechanical Engineering at the University of Brasilia, for providing access to the fluidization equipment.

References

[1] Arias B, Pevida C, Fermoso J, Plaza MG, Rubier F, Pisa JJ. Influence of torrefaction on the grindability and reactivity of woody biomass. Fuel Process Technol 2008;89:169–75.
[2] Bergman PCA, Kiel JHA. Torrefaction for biomass upgrading. In: 14th European biomass conference & exhibition, Paris, France; 2005. p. 8.
[3] Rousset P, Lapierre C, Perré P, Quirino W. Effect of extreme thermal treatment on lignins in spruce and beech wood. Ann Forest Sci 2009;66.
[4] Li J, Gifford J. Evaluation of woody biomass torrefaction. Rotorua, New Zealand: Forest Research; 2001.
[5] Commandré JM, Rousset P, Lesueur G, Leboeuf A, Chafchaouni L. Torrefaction of biomass: influence of operating conditions on products. In: WasteEng2010 conference, Beijing, China; 2010.
[6] Repellin V, Govin A, Rolland M, Guyonnet R. Energy requirement for fine grinding of torrefied wood. Biomass Bioenergy 2010;34:923–30.
[7] Chase G. Fluidization. In: Lecture notes. <http://coel.ecgf.uakron.edu/~chem/fclty/chase/SolidsNotes5.PDF>, University of Akron; 2001.
[8] Cui H, Grace JR. Fluidization of biomass particles: a review of experimental multiphase flow aspects. Chem Eng Sci 2007;62:45–55.
[9] Prins MJ, Ptasinski KJ, Janssen FJJG. More efficient biomass gasification via torrefaction. Energy 2006;31:3458–70.
[10] Svoboda K, Pohorelý M, Hartman M, Martinec J. Pretreatment and feeding of biomass for pressurized entrained flow gasification. Fuel Process Technol 2009;90:629–35.
[11] Almeida G, Brito JO, Perré P. Alterations in energy properties of eucalyptus wood and bark subjected to torrefaction: the potential of mass loss as a synthetic indicator. Bioresour Technol 2010;101:9778–84.
[12] Brosse N, El Hage R, Chaouch M, Pétrissans M, Dumarçay S, Gérardin P. Investigation of the chemical modifications of beech wood lignin during heat treatment. Polym Degrad Stabil 2010;95:1721–6.
[13] Phanphanich M, Mani S. Impact of torrefaction on the grindability and fuel characteristics of forest biomass. Bioresour Technol 2010. http://dx.doi.org/10.1016/j.biortech.2010.08.028.
[14] Nguila Inari G, Petrissans M, Gerardin P. Chemical reactivity of heat-treated wood. Wood Sci Technol 2007;41:157–68.
[15] Abdullah MZ, Husain Z, Yin Pong SL. Analysis of cold flow fluidization test results for various biomass fuels. Biomass Bioenergy 2003;24:487–94.
[16] Rodrigues TO, Rousset P. Effects of torrefaction on energy properties of *Eucalyptus grandis* wood. Cerne, Lavras 2009;15:446–52.
[17] Arffa R, Chan D, Patel R, Shukla A. Examination of the Ergun equation: flow through packed beds. In: 06-363 Transport Process Lab., Carnegie Mellon University, Pittsburgh, PA 15213; 2005.
[18] Ergun S. Fluid flow through packed columns. Chem Eng Prog 1952;48(2):89–94.
[19] Patankar SV. Numerical heat transfer and fluid flow, New York; 1980.
[20] Zhang Y, Jin B, Zhong W. Fluidization, mixing and segregation of a biomass–sand mixture in a fluidized bed. Int J Chem React Eng 2008;6:1–25.
[21] Sahai H, Ageel MI. The analysis of variance, Boston; 2000.
[22] http://www.xlstat.com. XLSTAT. Data analysis and statistics software for Microsoft Excel. In: Addinsoft, editor. Addinsoft, Paris, France; 2011.
[23] Schär C. A generalization of Bernoulli's theorem. J Atmos Sci 1993;50:1437–43.
[24] Leon MA, Dutta A. Fluidization characteristics of rice husk in a bubbling fluidized bed. The Can J Chem Eng 2010;88:18–22.
[25] Miao Q, Wang C, Wu C, Yin X, Zhu J. Fluidization of sawdust in a cold model circulating fluidized bed: Experimental study. Chem Eng J 2011;167:335–41.